ELSEVIER

Journal of Nuclear Materials 283–287 (2000) 1292–1296

journal of nuclear materials

www.elsevier.nl/locate/jnucmat

The oxidation kinetics of Incoloy 800 and its deuterium permeation behavior

A. Perujo [a,*], J. Reimann [b], H. Feuerstein [b], B. Mancinelli [a]

[a] *E.C., Joint Research Centre-Ispra Site, Environment Institute, 21020 Ispra (Va), Italy*
[b] *Forschungszentrum Karlsruhe GmbH, P.O. Box 3640, D-76021 Karlsruhe, Germany*

Abstract

Tritium permeation through the steam generator of the Helium-Cooled Pebble Bed Blanket (HCPB) concept can be strongly reduced by natural oxides formed on the Incoloy 800 tubes. This paper presents the results of different experiments with various deuterium to humidity ratios (p_{H_2O}/p_{D_2} from 300 vppm to 30%). All experiments show that Incoloy 800 readily oxidizes and that permeation reduction factors (PRF) of at least 100 are easily obtained for typical blanket conditions. The measured PRF values are explained in terms of the type and thickness of the oxides on the Incoloy surface. The observed reduction in permeation is very favorable for the design of the HCPB blanket system in order to reduce the amount of hydrogen needed for isotope swamping and hence, reducing the size of the tritium extraction system. © 2000 Elsevier Science B.V. All rights reserved.

1. Introduction

Permeation of tritium through structural materials is one of the most important operational and safety issues for fusion reactors. The amount of tritium that is acceptable to be released to the environment during usual operation is about 20 Ci/day. For the Helium-Cooled Pebble Bed blanket (HCPB) [1], tritium passes to the environment mainly by permeation from the helium coolant system through the Incoloy 800 steam generator walls into the steam cycle. Therefore, tritium permeation mechanisms through this material and its control are of large interest.

Detailed calculations have been performed to evaluate the amounts of tritium coming from different sources in the HCPB and finally, the tritium permeation rate through the steam generator was assessed [1]. The main tritium source was found to be the permeation through the first wall (FW) (it should be stressed that, pessimistically, a bare FW was assumed in [1]); the contribution from the purge system is only ≈0.8 g/day. It was calculated that the resulting permeation rate through the steam generator exceeded the acceptable release value, assuming bare material, but was reduced to below this value for a permeation reduction factor (PRF) of about 20 in the steam generator. A larger FW permeation rate could be compensated either by a significant increase of the tritium extraction system from the He coolant or by higher values of the PRF.

The values found in [1] correspond to a hydrogen addition of ≈18.8 and ≈37.7 kg/day, respectively, which are co-precipitated with the tritium of about ≈10 g/day in the extraction unit. These values significantly influence the design and operation of the extraction system. However, if PRF values significantly larger than 20 could be reached, then the required amount of hydrogen addition would be reduced thus reducing the size and operational costs of the system [2].

The main goal of the present investigations is the development of permeation barriers by in situ oxidation of the Incoloy 800 surface. Similar works in the area of high-temperature gas-cooled reactors [3,4] have been performed, but they were concentrated on significantly higher hydrogen pressures and temperatures. The extrapolation of their results to HCPB conditions, which are characterized by steam generator material temperatures

---

[*] Corresponding author. Tel.: +39-0332 789 062; fax: +39-0332 785 640.
E-mail address: adolfo.perujo@jrc.it (A. Perujo).

0022-3115/00/$ - see front matter © 2000 Elsevier Science B.V. All rights reserved.
PII: S0022-3115(00)00180-X

between 250°C and 500°C and hydrogen pressures far below one bar, is at best uncertain.

2. Experimental

The two methods chosen for the permeation measurements during the current investigation were gas-phase techniques. The first method (isovolumetric permeation, used at JRC [5]) consists of evacuating the apparatus to an ultra-high vacuum (UHV), so that both sides of a sample are initially in contact with vacuum. Then, one side of the sample (the 'high pressure side') is instantaneously exposed to deuterium gas (99.7% pure) at a known, fixed pressure. Gas permeates through the sample and is released at the other side (the 'low pressure side'), where it causes a pressure rise in an initially evacuated, calibrated volume. The pressure rise is measured using a Baratron capacitance manometer with a full-scale reading of 100 Pa (1 mbar). Since the volume is calibrated, either the pressure rise could be converted into an amount of gas in moles permeating through unit area of the sample ($Q(t)$) or the rate of pressure rise could be converted into an amount of gas in moles permeating through unit area of the sample per second ($J(t)$) [5]. The system also has a quadrupole mass spectrometer to check for humidity content and gas purity. Deuterium, rather than hydrogen, was chosen for this study to avoid possible uncertainties posed by the hydrogen background of the apparatus.

In the second method, used at FZK, gases at atmospheric pressure are flowing to both sides of the membrane. The upstream gas contains D_2 at different partial pressures in Ar-6.0. The downstream gas is always Ar-6.0. Both gases are analyzed simultaneously with a HP5890 gas chromatograph with a mini-thermal conductivity detector. Permeation rates are obtained from changes in D_2 concentrations in the up and downstream gases.

Following bake-out under UHV conditions, the sensitivity of both methods enables the measurement of permeation fluxes down to about 10^{-10} mol m^{-2} s^{-1}.

In both experimental procedures, the humidity in the high-pressure side was controlled by passing the high purity gas through a humidifier (a mixture of oxalic acid/oxalic acid dihydrate 9:1). This mixture gives a well-defined H_2O partial pressure/temperature dependence (Fig. 1).

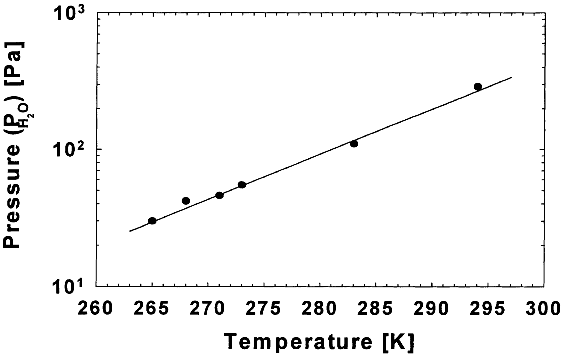

Fig. 1. Theoretical humidity at a given temperature (line) of the humidifier and that measured by gas chromatography (full dots).

The specimens consisted of 48-mm diameter disks of Incoloy 800 with 0.4, 0.8 or 1-mm thickness. The disks were cut from a sheet with the following nominal composition (wt.%): Ni 30.8, Cr 20.05, Mn 0.64, Ti 0.56, Si 0.46, Al 0.36, C 0.065, S 0.004 and Fe (balance). The specimen used in the FZK experimental runs was electropolished before its introduction in the experimental rig, while those specimens used at JRC were only chemically degreased and rinsed in water and ethanol to eliminate the traces left from the machining process. This is an important difference between both sets of specimens that might explain the different results obtained (see following sections).

3. Results and discussion

Initial measurements on the unoxidized specimen to obtain a reference measurement in the temperature range 423–773 K (150–500°C) were difficult to achieve due to the tendency of the specimen to readily oxidize above 520 K (250°C). In steels, the presence of Mn decreases their oxidation resistance. Wild [6] assigned this effect to the higher diffusivity of Mn as compared to Cr in Cr_2O_3 (two orders of magnitude at 1070 K). This was also observed by Stott and co-workers [7] in Fe–Cr alloys with different Mn concentrations. Therefore, the Incoloy 800 is easily oxidized even with the background humidity existing during these tests. Other authors [8–11] have found similar behavior for Incoloy 800 specimens. In particular, Bittner and co-workers [11] found Cr and Mn rich oxides after oxidation of as-received Incoloy tubes. However, iron oxides were predominant in the case of electropolished specimens. They also found that the different oxidation characteristics of the as-received and the electropolished specimens might be due to the presence of a thin oxide coating of Cr_2O_3 on the as-received material prior to oxidation; this could have inhibited the formation of iron oxides.

Oxidation is apparent due to the strong reduction of the permeation flux through the specimens as shown in Fig. 2, where the arrows indicate the sequence of measurements. With increasing exposure time and temperature, the permeation flux deviates increasingly from that of the bare material. The maximum PRF obtained in the JRC-Ispra experiments has been around four orders of magnitude at 485°C.

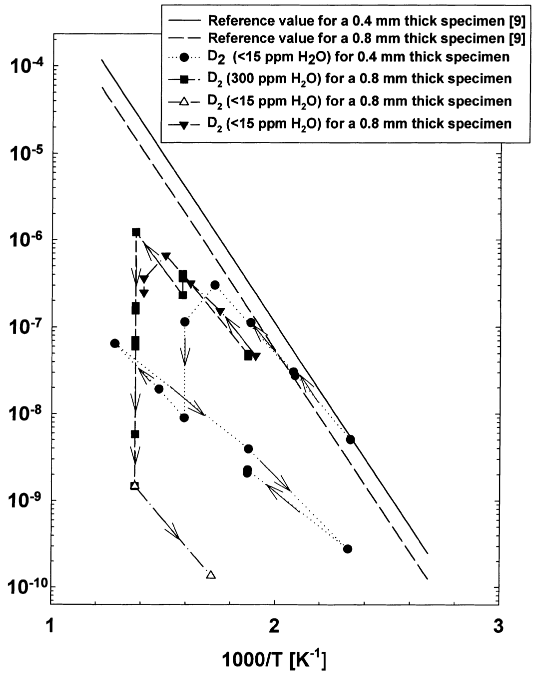

Fig. 2. Arrhenius' plot of the permeation rate for two Incoloy 800 specimens with different humidity contents in the upstream side. The driving pressure was 100 kPa.

An important parameter to study is the kinetics of the oxidation process, because this will indicate the feasibility of using direct oxidation to form an efficient permeation barrier.

Fig. 3 depicts the changes of the permeating flux with time of exposure for different experimental conditions. These curves indicate the rate of change of the permeating deuterium flux and hence,by inference, the speed of oxide growth on the surface of the specimen. The JRC-Ispra data (curves 1, 5, 6 and 7 in Fig. 3) show an initial strong decrease of the permeation flux followed by a rather constant value for larger exposure times. The FZK data (curves 2, 3 and 4 in Fig. 3) do not exhibit this strong initial decrease; however, from the beginning the values are lower by a factor of about 100 than those of the bare material depicted in Fig. 2. Repeating the JRC-Ispra experiment with $p_{D_2} = 100$ kPa with a new specimen resulted in a similar result as in the first experiment, as shown in Fig. 3. The different tendencies may be attributed to a possible formation of different oxides on the surface of the two specimens tested in both installations and in particular, to the surface treatment of the specimens before their measurements (see section above). As Bittner and co-workers [11] found, electropolished specimens tend to form iron oxides that are less efficient as permeation barriers than Cr_2O_3. Secondary Neutral Mass Spectroscopy (SNMS) analysis of the 0.4-mm thick specimen tested in JRC-Ispra showed the presence of an oxide layer of about 100 nm with an enrichment of Mn, Cr and O in the first 30 nm. XPS analysis of the 0.8-mm thick specimen also indicated the presence of the same type of oxides on its surface. This confirms the presence of a mixed oxide of Cr–Mn (probably a spinel Cr_{3-x} Mn_xO_4) on the surface and its effectiveness as a permeation barrier. This is in agreement with the oxide ($MnCr_2O_4$) found by Strehlow and Savage [9] on the surface of their Incoloy 800 specimens.

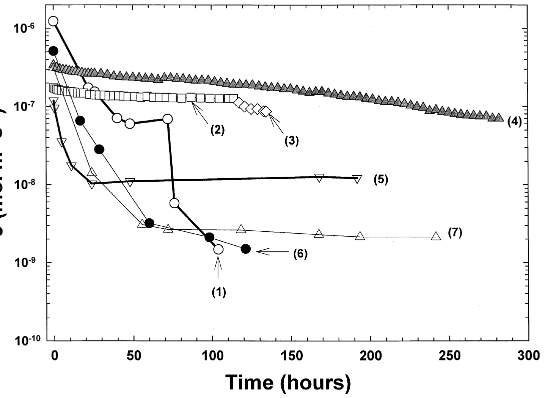

Fig. 3. Permeation rate as a function of the exposure time for different H_2O to D_2 ratios at different temperatures. (1) 100 kPa D_2, 450°C, 30 Pa H_2O; (2) 1.04 kPa D_2, 481°C, 30 Pa H_2O; (3) 1.04 kPa D_2, 481°C, 300 Pa H_2O; (4) 9.8 kPa D_2, 455°C, 100 Pa H_2O; (5) 20 kPa D_2, 250°C, 20 Pa H_2O; (6) 100 kPa D_2, 450°C, 30 Pa H_2O and (7) 5.5 kPa D_2, 450°C, 300 Pa H_2O.

4. Surface reaction rates constants

In the previous section, the ability of surface oxides in reducing the deuterium permeation flux through Incoloy 800 specimens has been established. This reduction is normally manifested by a change in the observed pressure dependence of the permeation flux from the half-power (i.e. diffusion limited regime), through greater than the half-power (i.e. mixed regime) to first power (i.e. surface limited regime). The deuterium transport kinetics in the two latest regimes is governed by the surface reaction constants and therefore, it is of interest to obtain them for this oxidized surface.

The steady state permeation rate, J, can be expressed by relatively simple analytical expressions (Eqs. (1) and (2)) for the two extreme behaviors; diffusion-limited and surface limited, respectively.

$$J(t) = \frac{DK_s\,p^{1/2}}{d}\left[1 + 2\sum_{n=1}^{\infty}(-1)^n\left(-D\frac{n^2\pi^2}{d^2}t\right)\right], \qquad (1)$$

$$J = \sigma k1\left[\frac{(\sigma k2)'}{(\sigma k2) + (\sigma k2)'}\right]p, \qquad (2)$$

where D is the diffusivity, K_S the Sieverts' constant, (the permeability $P = D\ K_S$), p is the pressure at the high-pressure side and $\sigma k_1, \sigma k_2$ (adsorption and recombination constants; high-pressure) $(\sigma k_1)'$ and $(\sigma k_2)'$ (adsorption and recombination constants; low-pressure) are the surface parameters of both specimen surfaces. Eq. (2) becomes $J = \sigma k_1/2p$ for a symmetrical membrane.

In the more general case where the permeation kinetics do not approach any of the two limits, an equation describing J in function of p is also needed. This can be obtained following the approach of Ali-Khan and co-workers [12]. They examined the intermediate regime and considered the following steps: molecular adsorption and desorption, surface dissociation and recombination, and diffusion within the lattice. In their treatment of the intermediate case they defined a dimensionless number W as follows:

$$W = \frac{\sigma k_1 d}{P} p^{1/2}(d) \tag{3}$$

and a reduced concentration C

$$C(0) = \frac{c(0)}{c_{\text{equilibrium}}} \tag{4}$$

where d is the thickness of the membrane and $x = d$ corresponds to the side facing the high-pressure side. W^2 can be interpreted as the reduced penetration flux. The other symbols have the usual meaning.

Following their description, the following expression can be derived which relates these two parameters:

$$W^2C^4(0) + 2WC^3(0) + 2C^2(0) = 1. \tag{5}$$

This is the general equation for the steady state permeation across a symmetrical membrane. When $W \ll 1$, Eq. (5) becomes $2C^2(0) = 1$ that implies $J = (\sigma k_1)/2p(d)$ and the permeation is directly proportional to the pressure. When $W \gg 1$ then we can get $C^2(0) = 1/W$ and using the definition of W and C, it can be seen that the permeation flux is directly proportional to the square root of the pressure.

A convenient way to determine the adsorption constant is to plot the ratio J/p as a function of W^2 (or p) and by fitting the experimental points to the theoretical curve one can obtain accurately the quantity $\sigma(k_1)$.

Following the above procedure, the surface reaction rate constant, σk_1, for Incoloy 800 has been obtained (σk_1 [mol m^{-2} s^{-1} Pa^{-1}] $= 4.494 \times 10^{-13}$ exp($-90680/RT$)). The Arrhenius plot of σk_1 for the oxidized specimen is compared with other works in Fig. 4. Because the specimen surfaces are not symmetric, the strict use of the above mathematical development for this case is not valid. In fact, the two surfaces are exposed to different conditions, namely, the surface facing the high-pressure side was in contact with a more humid gas than that of the downstream side where the gas is the one resulting from the permeation and therefore dryer. As a result of this, the values of σk_1 (see Fig. 4) showed an unusual large scattering that was further aggravated because during the measuring period, the membrane surface was still being oxidized. The values for σk_2 can be obtained using the following relation:

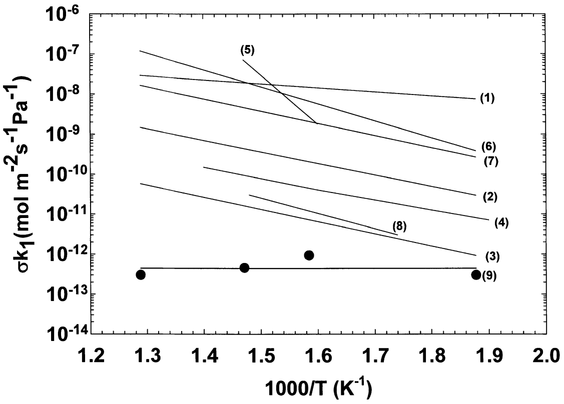

Fig. 4. Arrhenius plot of the measured surface rate constant σk_1 compared with other published data. (1) D_2-bare Manet II system [13]; (2) and (3) two different D_2-oxidized Manet systems [13,14]; (4) D_2–Inconel 600 system [15]; (5) H_2–St 60 system [12]; (6) H_2–316SS system (ion beam cleaned) [16]; (7) H_2–316SS system (both surfaces oxidized) [16]; (8) D_2–304 SS system [17] and (9) D_2–Incoloy 800 system (this work).

$$(\sigma k_1) = (\sigma k_2)K_s^2, \quad (\sigma k_1)' = (\sigma k_2)'K_s^2.$$

Further refining of the surface parameters can be obtained considering separately the contribution of the two surfaces by taking into consideration either the direct or reverse permeation fluxes.

5. Conclusions

In all experiments, a large reduction of the permeation flux is found compared with the values of the unoxidized materials [9]. The reduction factors are about 100 for initially electropolished specimens (FZK) and about one order of magnitude larger for the JRC-Ispra specimens that were initially chemically cleaned. The differences in the observed reduction factors between the two sets of specimens have been related to their initial surface cleaning procedure and consequently, to the different initial surface oxides (iron oxide and mixed chromium–manganese oxides, respectively).

The present experiments were performed in a static system, i.e. without mechanical cyclic loads. Previous cyclic loading experiments with Manet probes [18] have shown that the self-healing effect (oxidation of mechanically produced cracks) is very fast. Compared to Manet, oxide layers build up faster on Incoloy 800 surfaces. Therefore, no significant deterioration from thermomechanical cycling is to be expected.

At present, this experimental program has been terminated because it was shown that the presence of H_2O in the primary side of the Incoloy 800 steam generator will easily form natural oxide layers to such an extent that the tritium permeation rates in the blanket can be reduced to acceptable values.

In order to provide more detailed data, more experiments with various p_{H_2O}/p_{H_2O} ratios and under mechanical cycling are needed. An interesting aspect of any future work will be the investigation of the effect of a large hydrogen pressure on the downstream side. This case might be relevant for the steam generator if on the waterside, a significant amount of hydrogen exists which may influence the tritium recombination mechanism.

Currently, however, there is no need to perform these detailed experiments at this stage. As the designs of various blanket concepts are still under development, these tests will only be required prior to the design and construction of any large scale integrated experiments (i.e. ITER test blanket modules).

References

[1] L. Berardinuci, M. Dalle Donne, in: Proceedings of the SOFT, Lisbon, 16–20 September, 1996, Fus. Technol. (1996) 1427.

[2] H. Albrecht, E. Hutter, in: Proceedings of the Fifth International Symposium on Fusion Nuclear Technol., Rome, 19–24 September, 1999, to be published.

[3] J.T. Bell, J.D. Redman, 14th Intersoc. Energy Conservation Engineering Conference, Boston, USA, August 1979.

[4] H.D. Röhrig, R. Hecker, J. Blumensaat, J. Schäfer, Nucl. Eng. Des. 34 (1975) 157.

[5] A. Perujo, K.S. Forcey, Fus. Eng. Des. 28 (1995) 252.

[6] R.K. Wild, Corros. Sci. 17 (1977) 87.

[7] F.H. Stott, F.I. Wei, C.A. Enahoro, Werkst. Korros. 40 (1989) 198.

[8] J.T. Bell, J.D. Redman, H.F. Bittner, W.H. Christie, in: Proceedings of the Third Topical Meeting on the Technology of Controlled Nuclear Fusion vol. 2, 1978, p. 757.

[9] R.A. Strehlow, H.C. Savage, Nucl. Technol. 22 (1974) 127.

[10] R.A. Strehlow, H.C. Savage, J. Nucl. Mater. 53 (1974) 323.

[11] H.F. Bittner, J.T. Bell, J.D. Redman, W.H. Christie, R.E. Eby, Met. Trans. A 11A (1980) 783.

[12] I. Ali-Khan, K.J. Dietz, F. Waelbroeck, P. Wiendhold, J. Nucl. Mater. 76&77 (1978) 337.

[13] E. Serra, A. Perujo, J. Nucl. Mater. 240 (1997) 215.

[14] E. Serra, A. Perujo, J. Nucl. Mater. 223 (1995) 157.

[15] E. Rota, F. Waelbroeck, P. Wienhold, J. Winter, J. Nucl. Mater. 111&112 (1982) 233.

[16] D.M. Grant, D.L. Cumming, D.A. Blackburn, J. Nucl. Mater. 152 (1988) 139.

[17] M. Braun, B. Emmoth, F. Waelbroeck, P. Wiendhold, J. Nucl. Mater. 93&94 (1980) 861.

[18] A. Perujo, H. Kolbe, J. Nucl. Mater. 258–263 (1998) 582.